



HAL
open science

An integrated approach to characterize liquid leakage through metal contact seal

Christophe Marie, Didier Lasseux, Hassan Zahouani, Philippe Sainsot

► To cite this version:

Christophe Marie, Didier Lasseux, Hassan Zahouani, Philippe Sainsot. An integrated approach to characterize liquid leakage through metal contact seal. *European Journal of Mechanical and Environmental Engineering*, 2003, 48 (2), pp.81-86. hal-03827921

HAL Id: hal-03827921

<https://hal.science/hal-03827921>

Submitted on 2 Dec 2022

HAL is a multi-disciplinary open access archive for the deposit and dissemination of scientific research documents, whether they are published or not. The documents may come from teaching and research institutions in France or abroad, or from public or private research centers.

L'archive ouverte pluridisciplinaire **HAL**, est destinée au dépôt et à la diffusion de documents scientifiques de niveau recherche, publiés ou non, émanant des établissements d'enseignement et de recherche français ou étrangers, des laboratoires publics ou privés.



Distributed under a Creative Commons Attribution 4.0 International License

An integrated Approach to Characterize Liquid Leakage Through Metal Contact Seal

C. Marie¹, D. Lasseux¹, H Zahouani² and P. Sainsot³

¹ LEPT-ENSAM Esplanade des Arts et Métiers, 33405 TALENCE Cedex France
Tel : +33 (0) 556 845 400, Fax : +33 (0) 556 845 436

² LTDS ECL BP 163 - 36, Av. G. Collongue, 69131 ECULLY Cedex France
Tel : +33 (0) 472 186 286, Fax : +33 (0) 478 433 383

³ LMC INSA Lyon20, Av. A. Einstein, 69621 VILLEURBANNE Cedex France
Tel : +33 (0) 472 438 942, Fax : +33 (0) 478 890 980

E-mail : marie@lept-ensam.u-bordeaux.fr lasseux@lept-ensam.u-bordeaux.fr
hassan.zahouani@ec-lyon.fr sainsot@lmc.insa-lyon.fr

Abstract

Static seal is of major concern in spatial technology and because of severe thermodynamic conditions, direct metal/metal contact is often used. This work is a contribution to the study of liquid leakage through a rough metal contact resulting from the tightening of two machined surfaces. Our approach is based on experimental measurements of leak-rates on a model configuration close to a real design on the one hand and on theoretical developments for predictive estimates of leakage on the other hand.

Experiments are performed on turned metal samples reproducing the contact surface of a real metal seal. The sample is pressed against a sapphire surface under a controlled contact pressure using a specific experimental set-up. Leak tests are carried out with a liquid and leak-rate is measured versus liquid pressure and contact load using gas chromatography. Starting from the initial topology of the surface, elastic and plastic deformations are computed applying contact pressures corresponding to the ones used in the experiment. Computed deformed surfaces are further employed to form the aperture field on a representative part of the contact on which flow computation is performed. Assuming the flow to be exclusively pressure driven, the equivalent "permeability" of the contact is computed using the local Reynolds approximation classically employed for flow in fracture with slowly varying aperture. Experimental results are commented and compared to predictions.

Keywords: Static seal, liquid leakage, metal contact, permeability, leak-rate measurement, Reynolds equation

1 Introduction

Metal gaskets are commonly used for spatial and nuclear applications, whenever severe thermodynamic conditions are expected. In such cases, the use of rubber sealant is not allowed, and seal is performed by a direct metal/metal contact. This work is a contribution to the study of liquid leakage through a rough metal contact resulting from the tightening of two machined surfaces.

Very few papers are reporting study of metal seals in the literature. In an experimental work, Yanagisawa and al. [1] studied the influence of tightening on gas leakage (air or helium), for a « C seal ». The leak-rate was measured using a "water bubble" method, for moderate loads. Resulting deformations of the gasket under load and microscopic contact areas were investigated too but no leak-rate predictions were proposed. In a previous work [2], the important role of a lead-coating layer was demonstrated, during experiments at ambient and cryogenic temperatures (70K). The influence of the type of machining was investigated experimentally by

Matsuzaki and Kazamaki [3]. In this work, gas leak-rates obtained with turned, polished and lapped surfaces made of different materials like stainless or other alloy steels and copper were related to surface roughness and contact pressure. Nitrogen leak was detected by way of gas chromatography. Later, the same analysis was applied to the behaviour of knife edge seals [4].

In most cases, seal of metal gasket is investigated in very particular operating conditions from an empirical point of view. To improve the understanding of the entire process and finally help to a better design of the contact, an integrated approach is needed, including leak measurements, topology description at different scales of observation, deformation and flow computations based on various models. Our approach is an attempt to contribute to this task. On the one hand, experimental measurements of leak-rates were performed on a model configuration close to a real design and on the other hand theoretical developments for predictive estimates of leakage are proposed, including simulation of deformation and flow through the

contact. The experimental apparatus is described in part 2 of this paper, and leak-rate measurements are presented, for different values of fluid pressure and tightening. Leak-rate is characterized by the macroscopic permeability of the contact which is deduced from experimental data as a function of the contact pressure. In part 3, our theoretical description is presented and comparisons to experimental data are performed and discussed.

2 Experimental set-up and results

In this section, we first briefly describe the experimental device used to perform leak-rate measurements. Secondly, experimental results are presented. Finally, we indicate how the topology of the surface is recorded for subsequent simulations.

2.1 Description of the experimental apparatus

Classically, the contact between two rough surfaces can be viewed as being equivalent to the contact of a perfectly flat one and an imaginary rough surface having the following properties: roughness is the sum of roughnesses of the two initial surfaces, hardness is the one of the softest material and elasticity modulus is a combination of the two moduli ([5], [6]). The flat surface has an infinite hardness. Using this hypothesis, often referred to as "sum surface", allows us to replace the metal/metal contact under consideration by a contact between a rough metallic surface, and a flat surface, made of a harder material. Here, we study the contact configuration created by the tightening of a machined annular metallic surface against a sapphire window (see figure 1). The metallic surface, obtained by turning, was made of 316L stainless steel and had an area of 38mm^2 . Its average roughness is $Ra \approx 1.1\mu\text{m}$, which is comparable to a flange roughness. The Young modulus of the sapphire ($E=440\text{ GPa}$ at 300 K) is about two times greater than that of stainless steel. We consider the flat surface as a non deformable one in the rest of the work.

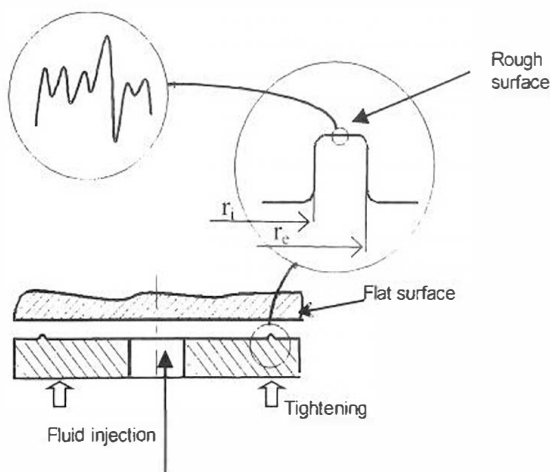


Fig 1. Configuration of the contact under study

The experimental set-up used in this work is schematically represented in figure 2. The metallic surface is pressed against the sapphire window using a hydraulic jack and tightening is controlled by a load cell. The fluid for which leakage is measured is stored in a tank axially connected to the contact and put under pressure using nitrogen. The pressurized fluid -or solute- leaks through the contact, and is collected in a solvent. Leak-rate measurements were performed by measuring the mass of solute passing through the contact in the solvent, during a given period of time using gas chromatography [7]. In our experiments, the leaking fluid was 1-butanol while the collector solvent was ethanol. A flame ionization detector was used, ensuring a rapid and accurate measurement, with high sensibility. To improve accuracy of leak-rate measurement, an internal standard was added to the solvent [8]. Calibration curves obtained from measurements performed on standard samples within the proportioning range expected for leakage were carried out first. This calibration provides a direct relationship between the solute peak area on chromatograms and the mass of solute present in the sample. These measurements are repeatable with a relative standard deviation of 1 %. Tightening used in our experiments ranged from 3.8kN to 30.4kN corresponding to a nominal contact pressure (P_{ca}) between 100 and 800 MPa . Precision on tightening measurement was 75N . Solute pressure ranged from 1 to 30 bars and was measured using a pressure transducer with a precision of 60mbar . A coil in which temperature regulated water was flowing kept the leakage cell at 20°C .

2.2 Experimental results: influence of fluid pressure and nominal contact pressure

Experiments were performed from low to high tightening and leak-rate measurements were carried out every P_{ca} increment of 100MPa . This procedure avoids possible roughness plastic deformation at high loads which might otherwise remain during measurements at lower loads. Because expected leak rates are extremely low (sometimes less than $1\mu\text{g}/\text{min}$) a special attention must be addressed to the experimental protocol. For instance, excessive care must be taken for surfaces cleanness since trapped or adsorbed solute might be a source of error estimation of the leak-rate. Moreover, putting the solute under pressure at the beginning of the experiment tends to decrease tightening and this effect must be corrected by increasing the load of the corresponding value.

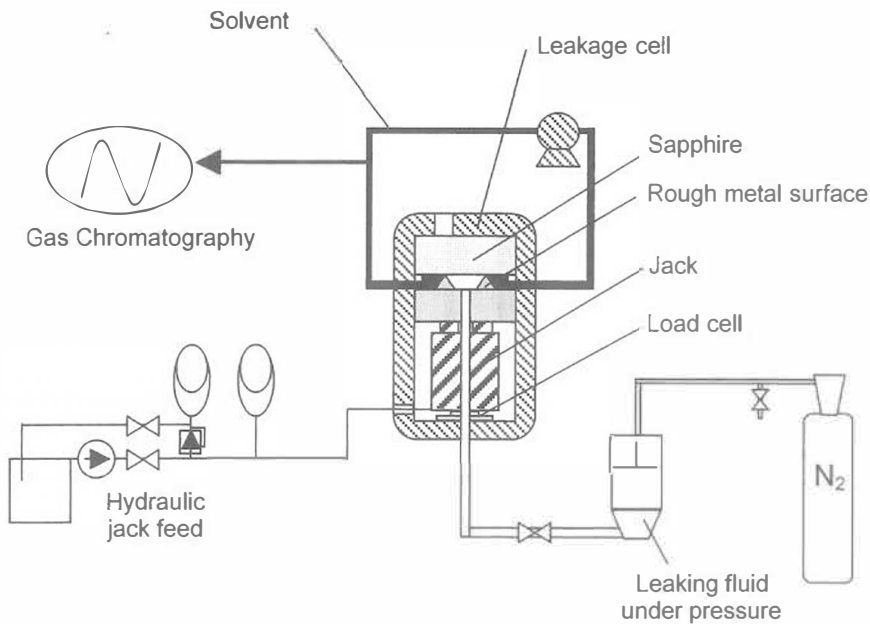


Fig 2. Description of the experimental apparatus

On figure 3, we have represented the evolution of the mass of butanol passing through the contact between the sapphire and the metallic surface -referred to as B- versus time, for three different pressure drops: 5, 10 and 15 bars. The pressure drop corresponds to the difference between the solute pressure P_i in the tank and the outer pressure P_e in the solvent which remains very close to atmospheric pressure since flow of the solvent is very slow. Experiments reported in figure 3 were obtained with a nominal contact pressure equal to 300 MPa. Measurements were performed over roughly 100 minutes.

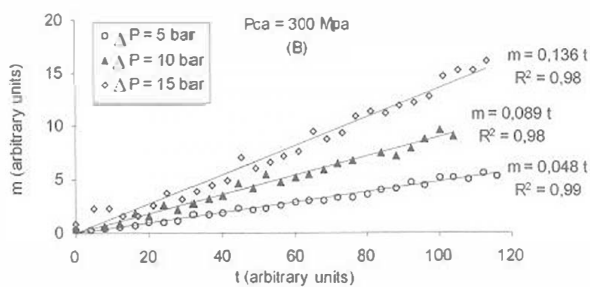


Fig 3. Leak-rate measurement, contact B

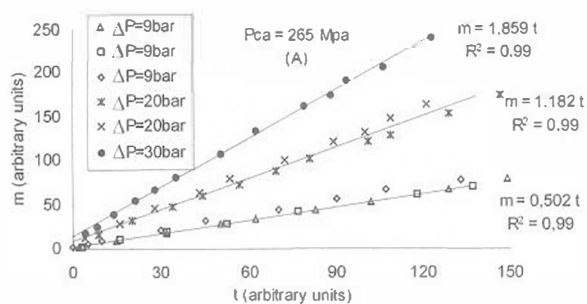


Fig 4. Leak-rate measurement, contact A

This figure clearly highlights the very good linearity of the mass of leaking fluid versus time [9]. Moreover, as shown on figure 4 representing results obtained with

another turned surface -referred to as A ; $R_a=0,5\mu m$ -, the reproducibility is excellent since less than 10% of variation is observed between two measurements performed under identical experimental conditions (tightening and fluid pressure) [10]. This indicates that the mass leak-rate through the contact can be derived from the slope of trend lines on these data for each value of tightening and pressure drop. Results obtained with this procedure applied to data obtained on surface B are depicted in figure 5 where we have represented the mass leak rate versus pressure drop for four values of nominal contact pressure.

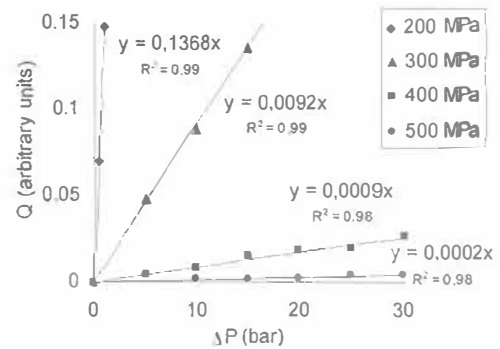


Fig 5. Leak-rate versus pressure drop through the contact for different values of tightening. Contact B

Again, one can observe that leak-rate depends linearly on the pressure drop with excellent correlation coefficients. In addition, the method used in the present work reveals to be extremely sensitive to detect liquid leakage, and is actually as sensitive as mass spectrometer method.

The linearity between mass leak rate and pressure drop allows describing the flow through the annular contact by Reynolds' law classically used for flow in fractures

$$[11]: \quad \frac{Q}{2\pi} = \frac{K}{\mu} \frac{(P_i - P_e)}{\ln(r_o / r_i)} \quad (1)$$

In this relationship, Q is the volume leak-rate, r_e and r_i the external and internal radii of the contact, K the contact permeability -or transmissivity- (in m^3), and μ the dynamic viscosity of the leaking fluid. Permeability of the contact can then be estimated from slopes of the trend lines in figure 5 and equation (1). In figure 6, we have represented the evolution of the permeability of the contact versus the nominal contact pressure and we have reported two series of experiments repeated on two similar surfaces B1 and B2 obtained with the same machining parameters. Again, an excellent reproducibility is obtained.

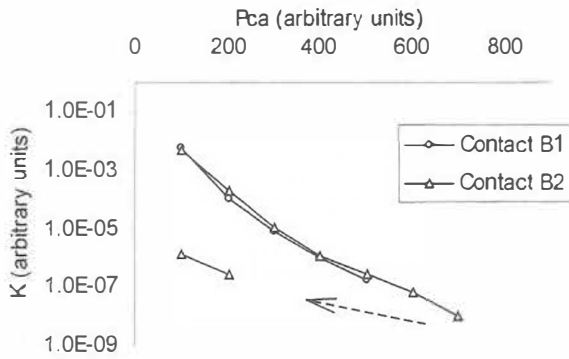


Fig 6. Contact permeability versus tightening for two similar rough surfaces B1 and B2

This result clearly highlights the important influence of P_{ca} on permeability of the contact since permeability varies over approximately seven orders of magnitude for pressure contact varying between 100 and 700 MPa following roughly a power-law [12]. For $P_{ca}=800$ MPa, no leakage was detected. This indicates that the experimental percolation threshold can be located between 700 and 800 MPa. When P_{ca} is gradually decreased from 800 to 100 MPa, a complete different behaviour of permeability is observed. Indeed, no leakage is detected between 800 and 300 MPa (see arrow on figure 6). Leak-rates measured at 200 and 100 MPa are much weaker than those measured while increasing the nominal pressure contact. This must be the proof of permanent deformations of contact roughnesses in the plastic domain remaining during the contact pressure release.

2.3 Topology description

Description of the contact topology is the starting point to apply physical models of surface deformation and fluid flow. In fact, this consists in the correct description of the aperture field resulting from the contact between the rough and flat surfaces in the "sum surface" context. The problem under consideration involves several scales corresponding to defects of very different characteristic lengths. In the present work, a simplified description of the topology is proposed based on only two scales of description. The first one corresponds to a description of roughness. Although this term does not refer to a precise definition of a characteristic length -a thorough discussion of this problem is beyond the scope of this paper- we assume here that it corresponds to the thread of the spiral resulting from turning. The second one also imposed by the machining process, corresponds to defects resulting from machine and tool vibrations and will be referred to as "form defects" in the following.

Surface roughness measurements were performed using a white light interferometer. This setup allows obtaining a topology description on part of the metallic surface, which size is typically of the order of $100 \times 100 \mu m^2$. The vertical resolution of this technique is 2 nm while the x-y resolution is 0.1 to 1 μm . In figure 7 we have represented the initial surface topology of a part of the metallic surface B. Dimensions of the scanned part are 230 μm along x, and 300 μm along y. In the y directions, one can observe tool marks corresponding to characteristic grooves of turned surfaces which wave length and amplitude are roughly 50 μm and 4 μm respectively.

Form defects were detected using classical flatness measurement using conventional fingering (Talyron). The finger records the altitude variation of the surface all over the circumference of the contact (see figure 8).

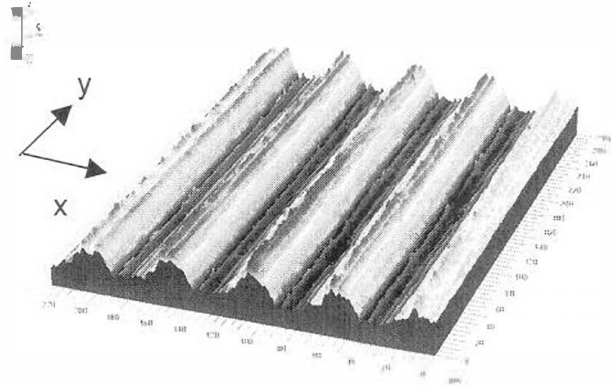


Fig 7. Interferometric image of the rough surface of the contact, surface B1

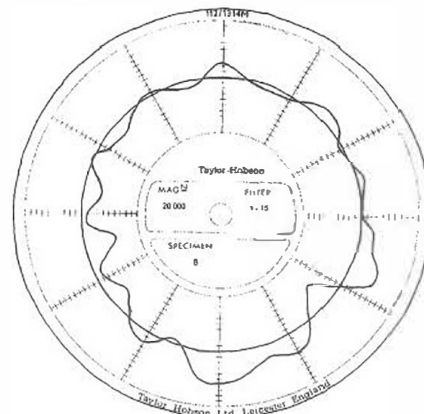


Fig 8. Flatness measurement on the rough surface B1

3 Theoretical description and comparison to experimental data

Starting from the initial topology of the surface, elasto-plastic and plastic deformations are computed applying contact pressures corresponding to the ones used in the experiment. The first elasto-plastic deformation model [13] is based on the calculation of the contact pressure in the elastic domain, using the Boussinesq approximation. When local contact pressure is greater than the yield stress of the material, plasticity law is applied, and local plastic deformation is determined in order to satisfy the overall force balance. The second elasto-plastic deformation model [14] makes use of Hertz' contact theory in order to determine the local contact area on top of each asperity. The deformation domain of each asperity is then determined, and the

pressure contact and contact area values are corrected if necessary, according to [15] and [16]. The third simplified plastic model consists in pure erosion on top of the asperities, so that the sum of the local forces (defined as yield stress multiplied by the local contact area) is equal to P_{ca} .

Assuming the flow to be exclusively pressure driven, the equivalent permeability of the contact is computed using the local Reynolds approximation (lubrication) classically employed for flow in fracture with slowly varying aperture. At the scale of roughness, the Reynolds model is a 2D one and can be written as:

$$\nabla \cdot \mathbf{q}(x, y) = 0 \quad (2)$$

$$\mathbf{q}(x, y) = -\frac{h^3(x, y)}{12\mu} \nabla p(x, y) \quad (3)$$

where \mathbf{q} is the local volume flow-rate per local unit width, $h(x, y)$ is the local aperture of the contact, μ is the dynamic viscosity of the fluid and ∇p is the local pressure gradient. This equation is formally equivalent to local Darcy's law and for this reason the model at the scale of the contact can be derived in a straightforward manner using results available in the literature on averaging performed on Darcy's law ([17] and [18]). Averaging the local Reynolds model leads to:

$$\nabla \cdot \langle \mathbf{q} \rangle = 0 \quad (4)$$

$$\langle \mathbf{q} \rangle = -\frac{\mathbf{K}^*}{\mu} \cdot \nabla \langle p \rangle^\beta \quad (5)$$

where \mathbf{K}^* is the theoretical macroscopic permeability tensor of the contact, $\langle \mathbf{q} \rangle$ is the volume leak-rate at the contact scale and $\nabla \langle p \rangle^\beta$ is the pressure gradient in the fluid, applied to the contact. The macroscopic permeability, \mathbf{K}^* , can be evaluated from the solution of a pure geometrical problem on a representative part of the contact.

In order to select a deformation model among the three, each of them was applied on the part of the rough surface represented in figure 7 using a flat and non deformable surface (sapphire) tightened at $P_{ca}=200$ MPa. Fluid flow simulation was then performed on these aperture fields in order to identify the permeability. The term of the tensor corresponding to the x direction being zero in each case, the comparison is performed on the permeability in the y direction. This comparison, summarized in table 1, shows a very small influence of the deformation model on permeability results.

	K_{yy}^* (μm^3)
Elasto-plastic deformation model [13]	0.94
Elasto-plastic deformation model [14]	1.12
Plastic deformation	1.03

Table 1 Comparison of permeability computed from different deformation models

As a consequence, the simple plastic model (erosion) is further used on the entire contact generated from the simplified description of the topology using the two scales mentioned above.

Since a complete description of the aperture field from direct measurement at the scale of roughness over the whole metallic surface can not be envisaged, the generation was performed by combining i) a radial profile extracted in the x direction from the set of data represented in figure 7, ii) the profile including form defects obtained on the overall circumference. In addition, because the width of the contact ($r_e-r_i=0.3\text{mm}$) is much smaller than its mean radius ($(r_e+r_i)/2=20\text{mm}$), this combination is performed in cartesian coordinates using profiles of figures 9 and 10. This leads to the surface represented in figure 11 and, on this figure, one has to keep in mind that periodicity must apply in the y direction to keep the original spiral-like structure. In particular, flow simulations were performed on this surface by applying pressure Dirichlet conditions in the x direction and periodic condition on both q and p in the y direction.

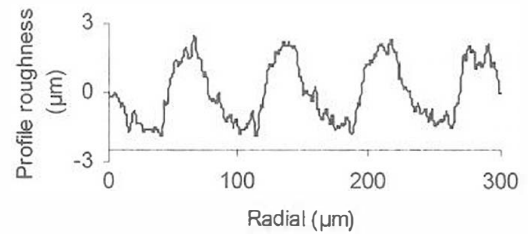


Fig 9. Radial profile extracted from figure 7

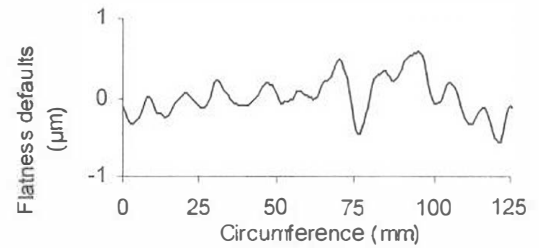


Fig 10. Cartesian representation of flatness measurement of figure 8

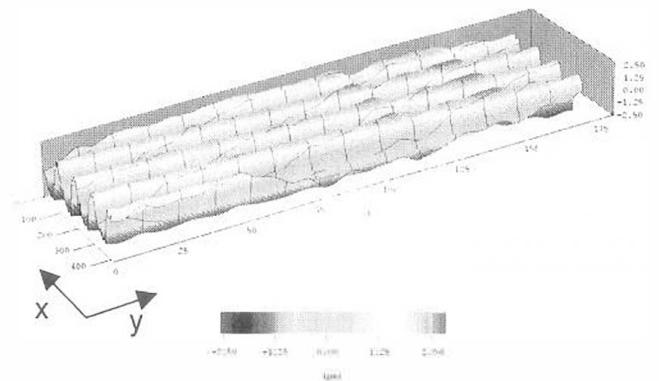


Fig 11. Complete generated surface B

Permeability was computed on aperture fields obtained from this surface on which the simple plastic deformation was applied for nominal contact pressure ranging from 100MPa to 700MPa using a flat non deformable surface. Our numerical results are represented in figure 12 along with the experimental data.

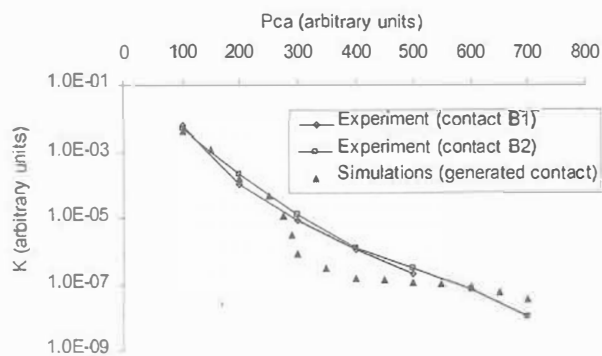


Fig 12. Comparison between theoretical and experimental results

The comparison shows a good general agreement between the experimental results and the theoretical approach. For relatively weak loads (100-250 MPa), a very good agreement is observed between prediction and experiments. In this case, numerical velocity fields indicate that leakage is radial and governed by the form defects highlighted in figure 10. For higher loads (500-700 MPa), the comparison remains satisfactory while simulations indicate that flow is purely circumferential, i.e. that fluid flow occurs in the spiral channel resulting from the turning process. Between the radial and circumferential regimes, numerical results show a clear transition region at intermediate loads (300-450 MPa) but this transition is not well identified on experimental data. However one must remind that, since the permeability varies with the cube of the contact aperture, the discrepancy result from an error in the aperture estimation on the order of a micron or less. A better agreement between experiment and numerical results could be expected in this transition zone by making use of a more sophisticated deformation model (elasto-plastic ones). Nevertheless, the prediction remains quite satisfactory.

4. Conclusion

In this work, an integrated approach was proposed to characterize liquid leakage through metal contact seal. The aperture field of the contact under load was computed from topology measurements at different scales of observation, using deformation models of roughness. Leakage was simulated using Reynolds approximation classical for flow in fracture. Results were compared over a wide range of tightening, to experimental data obtained with an original and specific experimental setup. Comparison between the two approaches is very satisfactory and highlights a radial and circumferential character of the leakage. Despite the stiffness of the problem, a better description of the aperture field would probably improve the estimation of the leakage in the transition between the two regimes.

Acknowledgement: This work was performed within the framework of a group of research including CNRS, CNES, EDF and SNECMA from which financial support is gratefully acknowledged.

References:

[1] Yanagisawa T., Sanada M., Koga T., and Hirabayashi H., (1991), The influence of

designing factors on the sealing performance of C-seal, *SAE Trans.*, 100, n°6, 651-657

[2] Yanagisawa T., Sanada M., Koga T. and Hirabayashi H., (1990), Fundamental study of the sealing performance of a C-shaped metal seal, *2nd International Symposium on Fluid Sealing*, La Baule, 18-20 September, 389-398

[3] Matsuzaki Y. and Kazamaki T., (1988), Effect of surface roughness on compressive stress of static seals, *JSME International Journal*, series III, 31, N°1.

[4] Matsuzaki Y., Hosokawa K. and Funabashi K., (1992), Effect of surface roughness on contact pressure of static seals, *JSME International Journal*, series III, 35, N°3.

[5] O'Callaghan P.W. and Probert S.D., (1987), Prediction and measurement of true areas of contact between solids, *Wear*, 120, 29-46.

[6] Francis H.A., (1977), Application of spherical indentation mechanics to reversible and irreversible contact between rough surfaces, *Wear*, 45, 221-269.

[7] Lasseux D. and Marie C. (2002), Appareil de mesure du débit de fuite d'un dispositif d'étanchéité, Patent n°0201930, february 15th 2002.

[8] Tranchant J., (1995), Manuel pratique de chromatographie en phase gazeuse, 4^{ème} édition, Masson, Paris.

[9] Marie C. and Lasseux D. (2001), Analyse expérimentale d'une fuite liquide au travers d'un contact statique métal/métal, 15^{ème} Congrès Français de Mécanique, Nancy, september 3-7.

[10] Marie C. and Lasseux D., (2002), Fuite monophasique dans un contact rugueux, *Journées CNES Jeunes Chercheurs*, Centre Spatial de Toulouse, april 24-26, 138-139.

[11] Zimmerman R.W., Kuzar S., and Bodvarsson G.S. (1991), Lubrication theory analysis of the permeability of rough-walled fractures, *International Journal of Rock Mechanics*, 28, n°4, 325-331.

[12] Marie C., (2002), Fuite monophasique au travers d'un contact rugueux : contribution à l'étude de l'étanchéité statique, *Thèse de doctorat*, Université Bordeaux 1.

[13] Sainsot P., (2001), Modélisation du contact rugueux revêtu, 15^{ème} Congrès Français de Mécanique, Nancy, september 3-7.

[14] Zahouani H., (2000), Rapport scientifique 2000, *GDR internal document*.

[15] Tabor D., (1951), The hardness of metals, *Oxford University Press*

[16] Johnson K.L., (1985), Contact mechanics, *Cambridge University Press*

[17] Quintard M. and Whitaker S., (1987), Ecoulement monophasique en milieu poreux : effet des hétérogénéités locales, *Journal de Mécanique théorique et appliquée*, 6, 691-726.

[18] Prat M., Plouraboué F. and Letalleur N., (2002), Averaged Reynolds equation for flow between rough surfaces in sliding motion, *Transport in Porous Media*, 48, 291-313.